Inorganic Chemistry

Article

pubs.acs.org/IC

The Effect of Synthetic Method and Annealing Temperature on Metal Site Preference in $Al_{1-x}Ga_xFeO_3$

James D. S. Walker and Andrew P. Grosvenor*

Department of Chemistry, University of Saskatchewan, Saskatoon, Saskatchewan, Canada, S7N 5C9

Supporting Information

ABSTRACT: Magnetoelectric materials couple both magnetic and electronic properties, making them attractive for use in multifunctional devices. The magnetoelectric $AFeO_3$ compounds ($Pna2_1$; A = Al, Ga) have received attention as the properties of the system depend on composition as well as the synthetic method used. $Al_{1-x}Ga_xFeO_3$ ($0 \leq x \leq 1$) was synthesized by the sol−gel and coprecipitation methods and studied by X-ray absorption near-edge spectroscopy (XANES). Al $L_{2,3}$-, Ga K-, and Fe K-edge XANES spectra were collected to examine how the average metal coordination number (CN) changes with the synthetic method. Al and Fe were found to prefer octahedral sites, while Ga prefers the tetrahedral site. It was found that composition played a larger role in determining site occupancies than synthetic method. Samples made by the sol−gel or ceramic methods (reported previously; Walker, J. D. S.; Grosvenor, A. P. *J. Solid State Chem.* **2013**, *197*, 147−153) showed smaller spectral changes than samples made via the coprecipitation method. This is attributed to greater ion mobility in samples synthesized via coprecipitation as the reactants do not have a long-range polymeric or oxide network during synthesis like samples synthesized via the sol−gel or ceramic method. Increasing annealing temperature increases the average coordination number of Al, and to a lesser extent Ga, while the average coordination number of Fe decreases. This study indicates that greater disorder is observed when the $Al_{1-x}Ga_xFeO_3$ compounds have high Al content, and when annealed at higher temperatures.

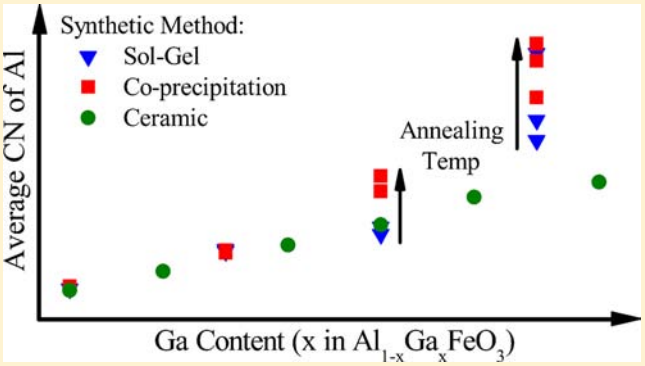

1. INTRODUCTION

Magnetoelectric compounds have received significant attention due to the complex coupling of the magnetic and electronic properties found in these materials.[1−3] This coupling has led to effects such as magnetically controlled second harmonic generation and optical frequency conversion in magnetoelectric photonic crystals being observed.[4,5] Unfortunately, these materials are rare due to the structural restrictions required for the coupling of magnetic and electronic properties.[1,2]

$AFeO_3$ compounds (A = Al, Ga) are magnetoelectric, in that they are ferrimagnetic and piezoelectric.[6,7] While it has been suggested that these materials are also ferroelectric, this property has not been decisively observed.[8] The $Al_{1-x}Ga_xFeO_3$ system ($0 \leq x \leq 1$) adopts a noncentrosymmetric orthorhombic crystal structure ($Pna2_1$; equivalent to $Pc2_1n$) with 4 distinct cation sites, and 6 distinct oxygen sites.[9,10] In the perfectly ordered structure (Figure 1), Fe occupies two highly distorted octahedral sites (Fe_1 and Fe_2) while Al and/or Ga occupy a nearly regular tetrahedral site and a third, less distorted octahedral site (A_1 and A_2, respectively).[9−11] While the piezoelectric properties are attributed to the noncentrosymmetric crystal structure, the ferrimagnetic properties are due to the amount of antisite disorder present, which is affected by the composition and synthetic method.[9,10,12−17] Since the Fe_1 sites are ferromagnetically coupled to each other, and antiferromagnetically coupled to the Fe_2 sites, if the system had no antisite disorder, then these materials would be antiferromagnetic.[10,15,18] However, this system experiences significant antisite disorder in which Fe partially occupies the A_1 and A_2 sites while Al and/or Ga partially occupies the Fe_1 and Fe_2 sites.[9,10,13,14,16−21] Fe ions present in the A_1 site couple ferromagnetically with the Fe ions occupying

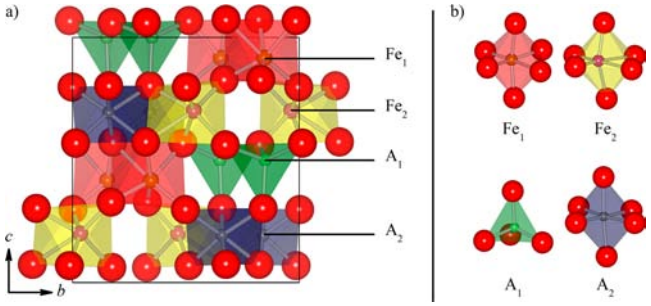

Figure 1. (a) The crystal structure of $AFeO_3$ (A = Al, Ga) is shown with the *a*-axis directed into the page. (b) The individual cation sites from $AFeO_3$ are presented. The octahedral Fe_1 and Fe_2 sites are significantly distorted, while the A_1 site is nearly tetrahedral and the octahedral A_2 site is slightly distorted.

Received: March 27, 2013
Published: July 18, 2013

   dx.doi.org/10.1021/ic4007636 | *Inorg. Chem.* 2013, 52, 8612−8620

the Fe_1 site and antiferromagnetically with Fe ions occupying the Fe_2 and A_2 sites.[9,18] Since the Fe ions are not evenly distributed across the four sites, the magnetic moments do not fully cancel, which gives rise to the observed ferrimagnetism of these materials.[9,22]

It has recently been shown that Fe occupies the tetrahedral site less with increasing Ga content in the $Al_{1-x}Ga_xFeO_3$ system, implying less antisite disorder in $GaFeO_3$ than in $AlFeO_3$.[17] That said, there are still unanswered questions regarding the effect of synthetic conditions on the $Al_{1-x}Ga_xFeO_3$ system. The synthetic method used to make these materials has been shown to significantly affect the magnetic transition temperature (T_c) of the $Al_{1-x}Ga_xFeO_3$ system.[20,21] In particular, the T_c of $GaFeO_3$ synthesized using sol−gel or flux techniques is between −15 and 10 °C (258 K and 283 K), while $GaFeO_3$ synthesized using high temperature ceramic methods has a T_c of approximately −70 °C (203 K).[6,21,23] Despite knowledge of these large changes in T_c, there have been few attempts to understand how the synthetic method affects metal site preference and the properties of the $Al_{1-x}Ga_xFeO_3$ system.[14,21,23] Unfortunately, accurate determination of site occupancies in the $Al_{1-x}Ga_xFeO_3$ system using common techniques such as X-ray or neutron diffraction data is difficult. In particular, it is difficult to perform Rietveld refinement of diffraction data from this system due to significant antisite disorder of multiple cations distributed across four crystallographic sites, while the O positions must be refined across six crystallographic sites.[14] X-ray absorption near-edge spectroscopy (XANES) is a tool well suited to examine site occupancies as it can probe the different coordination environments of a specific element.[17,24,25] In this study, Al $L_{2,3}$-, Ga K-, and Fe K-edge XANES spectra were collected from five stoichiometries of the $Al_{1-x}Ga_xFeO_3$ system prepared by either the sol−gel or coprecipitation method. These spectra were also compared to XANES spectra from samples synthesized via the ceramic method and reported in a previous study.[17] In addition, annealing studies were performed on multiple stoichiometries from the samples made via sol−gel and coprecipitation methods to better understand how temperature affects metal site preference in this system.

2. EXPERIMENTAL SECTION

2.1. Synthesis. $Al_{1-x}Ga_xFeO_3$ was synthesized using sol−gel and coprecipitation methods. In the sol−gel method, $Al_{1-x}Ga_xFeO_3$ (x = 0.00, 0.25, 0.50, 0.75, 1.00) was synthesized using a 0.2 mol/L solution of metal ions made through addition of stoichiometric amounts of $Al(NO_3)_3{\cdot}9H_2O$ (Alfa Aesar, 98%), $Ga(NO_3)_3{\cdot}xH_2O$ (Alfa Aesar, 99.9%), and $FeCl_3{\cdot}6H_2O$ (Alfa Aesar, 97.0%) to distilled water. The value of x was assumed to be 9 when calculating the mass of $Ga(NO_3)_3{\cdot}xH_2O$ used, as it is relatively close to an experimentally determined value.[26] It should be noted that this assumption will cause small deviations in the reported stoichiometry, but these deviations were not found to significantly affect the interpretation of the results. Ethylene glycol (Alfa Aesar, 99%) and citric acid monohydrate (EMD, 99%) were then added in equimolar amounts to the metal ion solution, to a concentration of 0.1 mol/L each. The solutions were heated to ∼80 °C to drive off the solvent, and were subsequently decomposed by heating to 600 °C in air. Samples were then ground, pelleted at 6 MPa, placed into an alumina crucible, and annealed at temperatures ranging from 900 to 1350 °C for ∼40 h, before being quench cooled in air.

In the coprecipitation method, $Al_{1-x}Ga_xFeO_3$ (x = 0.00, 0.25, 0.50, 0.75, 1.00) was made by weighing stoichiometric amounts of Al metal powder (Alfa Aesar, 99%), Ga_2O_3 (Alfa Aesar, 99.99%), and Fe_2O_3 (Alfa Aesar, 99.945%) into a beaker. Following this, 5−10 mL of 12.1 M HCl (Fischer Scientific, 37%) was added *very slowly* with heating and stirring to dissolve all of the reagents, resulting in a clear yellow solution. After the solution had cooled to room temperature, the metal ions were precipitated out of solution by titrating with 14.8 M NH_4OH (EMD Chemicals, 28.0−30.0%). The organic matter in the sample was then decomposed at 800 °C and subsequently annealed at temperatures ranging from 1000 to 1350 °C. It should be noted that higher annealing temperatures were required to form phase pure materials for Al rich compositions.[27,28]

All samples studied were determined to be phase pure by powder X-ray diffraction using a PANalytical Empyrean diffractometer and either Cu or Co $Ka_{1,2}$ radiation. Lattice constants for $Al_{1-x}Ga_xFeO_3$ were determined using the X'Pert HighScore Plus software from PANalytical and an orthorhombic model of the crystal structure ($Pna2_1$).[9,10,29] The lattice constants determined from samples synthesized at the same annealing temperature increased linearly with greater Ga content, in agreement with Vegard's law (see Tables S1 and S2 in the Supporting Information).[30,31] Figure 2 shows a diffraction pattern from samples produced via the sol−gel method, with the peak widths decreasing as the annealing temperature increased. This decrease in peak width indicates that the diffraction planes in the crystallites become more periodic resulting in more discretely defined atomic planes. That is, the samples become more crystalline with increasing annealing temperature. Diffraction patterns from samples synthesized via the coprecipitation method show a similar trend.

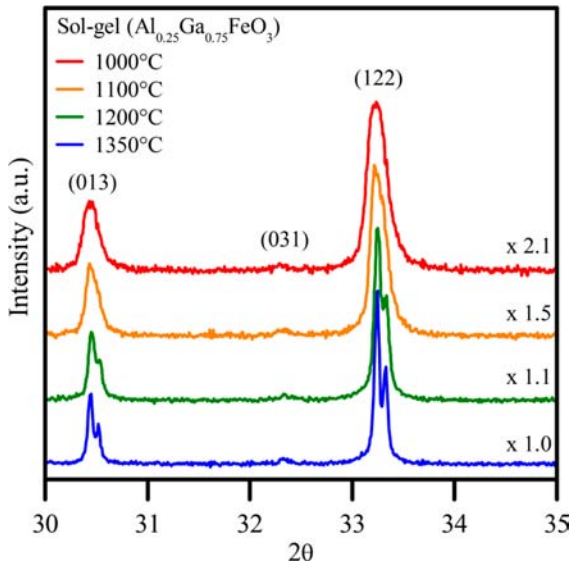

Figure 2. Powder X-ray diffraction patterns of $Al_{0.25}Ga_{0.75}FeO_3$ synthesized via the sol−gel method and annealed at different temperatures (using a Cu X-ray source) are shown. The patterns shown have been scaled to have the same (122) peak intensity (scaling factors are shown on the right-hand side). The peak widths decrease with increasing annealing temperature, indicating an increase in the crystallinity of the samples.

2.2. Al $L_{2,3}$-Edge XANES. The Al $L_{2,3}$-edge spectra were collected using the Variable Line Spacing Plane Grating Monochromator beamline (VLS PGM, 11ID-2) located at the Canadian Light Source (CLS).[32] Samples of $Al_{1-x}Ga_xFeO_3$ made by both sol−gel and coprecipitation methods were ground to a fine powder and mounted on C tape before being inserted into the vacuum chamber. Spectra were collected in fluorescence yield mode using a 0.025 eV step through the absorption edge and an entrance slit of 50 μm. The spectra were calibrated by collecting a spectrum from Al metal foil (Alfa Aesar, 99.99%) and setting the peak maximum of the first derivative of the spectrum to 72.55 eV.[33]

2.3. Ga and Fe K-Edge XANES. The Ga and Fe K-edge spectra were collected in transmission mode at the Pacific Northwest Consortium/X-ray Science Division Collaborative Access Team (PNC/XSD-CAT, Sector 20) bending magnet beamline (20-BM) located at the Advanced

dx.doi.org/10.1021/ic4007636 | Inorg. Chem. 2013, 52, 8612−8620

Photon Source (APS; Argonne National Laboratory) using a Si (111) crystal monochromator and ionization chambers filled with 100% $N_{2(g)}$.[34] Sample preparation consisted of spreading a thin layer of finely powdered material between two pieces of Kapton tape. Multiple sample layers were used to maximize absorption and sample uniformity.

Spectra from each sample were collected using a 0.2 eV step through the absorption edge for Ga, and a 0.15 eV step through the absorption edge for Fe. The spectra were calibrated by concurrently collecting spectra from a reference material and setting the peak maximum of the first derivative of the spectrum to a known value. Ga metal (sandwiched between two layers of Kapton tape) or Fe metal was used as a reference material and the spectra were calibrated to 10367 and 7112 eV for the Ga and Fe K-edge, respectively.[33] All spectra collected were calibrated, normalized, and analyzed using the Athena software program.[35]

3. RESULTS

3.1. Al $L_{2,3}$-Edge XANES. Al $L_{2,3}$-edge spectra are very sensitive to changes in the coordination environment around Al.[17,25] The lowest-energy features present in the Al $L_{2,3}$-edge spectra are primarily due to 2p → 3s transitions while higher energy features may involve 2p → 3d transitions.[36,37] In highly crystalline compounds containing Al with a single coordination number, the L_3- and L_2-edge features, which result from spin−orbit splitting, can be resolved.[17,37] In addition, the onset of the absorption edge energy from 6-coordinate Al compounds is shifted by ~1.5 eV to higher energy relative to 4-coordinate Al compounds (cf. Al $L_{2,3}$-edge spectra from Al_2O_3 and $AlPO_4$ in Figure 3a from ref 17).[17,37] When the electron is excited out of the 2p orbital, a core-hole is created which acts like a positive potential.[36] This potential is partially screened by the neighboring oxygen atoms which help stabilize the final state.[36] Thus, as the number of coordinating oxygen atoms increases from 4 to 6, the effective screening by the oxygen atoms increases, and the energy of the final state increases relative to the ground state resulting in the spectrum shifting to higher energy.[36,37] In compounds containing Al in multiple coordinate environments, the octahedral L_3- and tetrahedral L_2-edges overlap, and these features can no longer be resolved.[17,36,37] While the distinct L_3 and L_2 spin−orbit split peaks can no longer be individually observed, the transitions from 4- and 6-coordinate Al are represented by broad peaks occurring at different energies. That is, the lower energy peak corresponds to tetrahedrally coordinated Al, and the higher energy peak corresponds to octahedrally coordinated Al.[17,36,37]

The low energy region of the Al $L_{2,3}$-edge spectra from $Al_{1-x}Ga_xFeO_3$ synthesized by sol−gel and coprecipitation methods and annealed at 1350 °C is shown in Figure 3. Two peaks are present in each spectrum and are assigned in this study to represent 2p → 3s transitions resulting from the excitation of Al present in tetrahedral (peak T) and octahedral (peak O) coordination geometries. In the interpretation of the Al $L_{2,3}$-edge spectra presented here, peak O is exclusively assigned to representing a 2p → 3s transition from Al having an octahedral coordination; however, it is possible that this peak contains contributions from excitations from both tetrahedral and octahedral Al, especially as feature O is asymmetric in shape.[37] Despite this, and as will be shown below, a comparison of the intensities of peaks T and O provides an opportunity to study how the average Al coordination number changes depending on the composition of the material, and the synthetic method and annealing temperature used to produce the material. (The variation in the Al coordination determined through comparison of the intensity change of peaks T and O is corroborated in the following sections, which discuss the Ga K-edge spectra (section 3.2) and Fe K-edge spectra (section 3.3) from these $Al_{1-x}Ga_xFeO_3$ materials.) In both sets of Al $L_{2,3}$-edge XANES spectra presented in Figure 3, as the Ga content increases, the intensity of peak T (tetrahedral) decreases and the intensity of peak O (octahedral) increases. This indicates that Al occupies the octahedral sites *and* the tetrahedral site when the Ga content is low. With increasing Ga content, Al increasingly occupies the octahedral sites, and decreasingly occupies the tetrahedral site, which is consistent with previously published results on these materials synthesized using the ceramic method.[17]

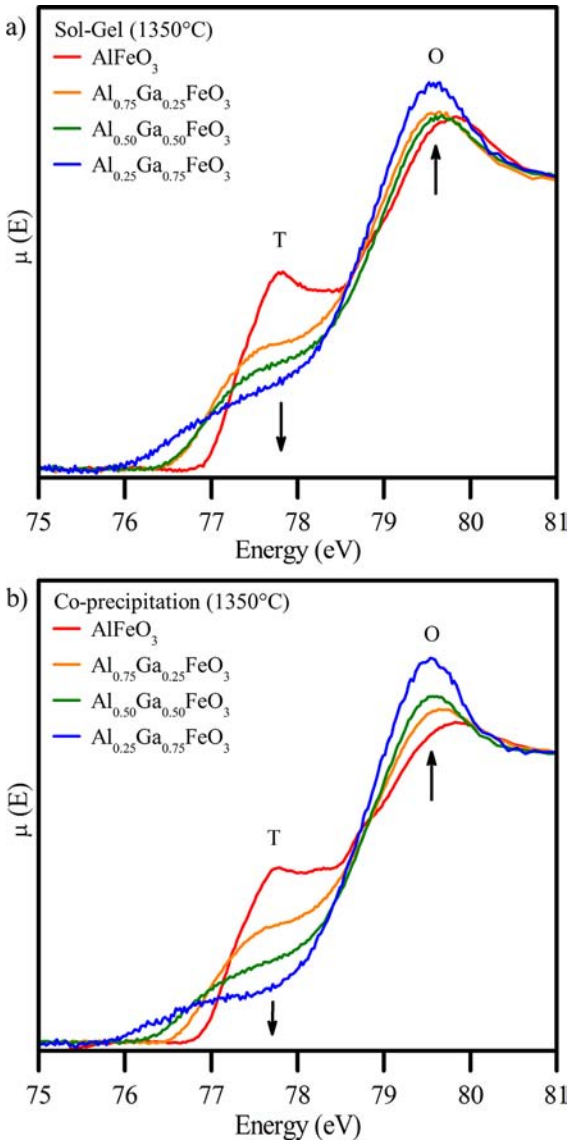

Figure 3. Normalized Al $L_{2,3}$-edge XANES spectra from $Al_{1-x}Ga_xFeO_3$ (x = 0.00, 0.25, 0.50, 0.75) synthesized using (a) the sol−gel method and (b) the coprecipitation method are presented. Both sets of spectra only show compounds annealed at 1350 °C. Arrows indicate the change in intensity with increasing Ga content. For both synthetic methods, Al occupies the octahedral sites as well as the tetrahedral sites when the Ga content is low. As the Ga content increases, Al decreasingly occupies the tetrahedral site (decrease in peak T intensity) and increasingly occupies the octahedral sites (increase in peak O intensity).

Al $L_{2,3}$-edge spectra from $Al_{0.25}Ga_{0.75}FeO_3$ synthesized by sol−gel and coprecipitation methods, and annealed at different temperatures, are presented in Figure 4 (see Figure S1 in the Supporting Information for additional stoichiometries). As the

dx.doi.org/10.1021/ic4007636 | Inorg. Chem. 2013, 52, 8612−8620

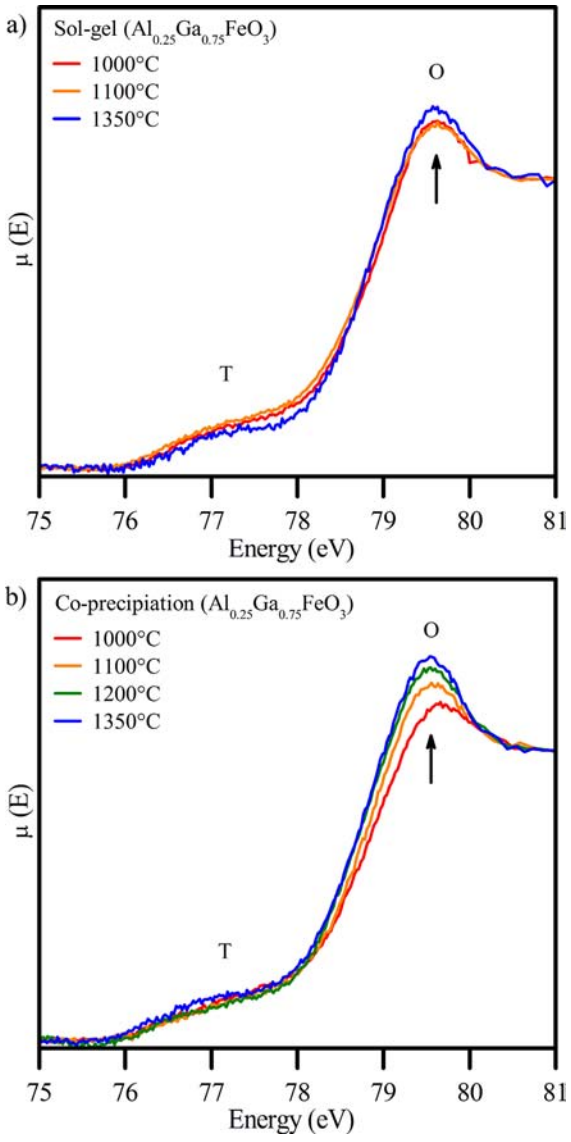

Figure 4. Normalized Al $L_{2,3}$-edge XANES spectra from $Al_{0.25}Ga_{0.75}FeO_3$ synthesized using (a) the sol−gel method and (b) the coprecipitation method, and annealed at multiple temperatures, are presented. Arrows indicate the change in intensity with increasing Ga content. For both synthetic methods, Al occupies the octahedral sites more with increasing annealing temperature. Any changes in the occupancy of the tetrahedral site are too small to detect when the Al concentration is this low, and no intensity change is observed.

changes with temperature are small, it is easier to see how the spectra change by comparing the ratio of the octahedral peak intensity to the tetrahedral peak intensity (feature O:feature T), as is shown in Figure 5 for all compositions and annealing temperatures (the data from Figure 5 is also summarized in Tables S3−S5 in the Supporting Information). In this plot, changes in composition result in larger changes in the peak intensity ratio than annealing temperature. This indicates that, in the $Al_{1-x}Ga_xFeO_3$ system, composition has a larger effect on the site preference of Al than annealing temperature. That said, the octahedral to tetrahedral peak intensity ratio does increase slightly with increasing annealing temperature when the Ga content is high ($x \geq 0.50$) and indicates that the amount of octahedrally coordinated Al increases relative to the amount of tetrahedrally coordinated Al. It should be noted that these ratios

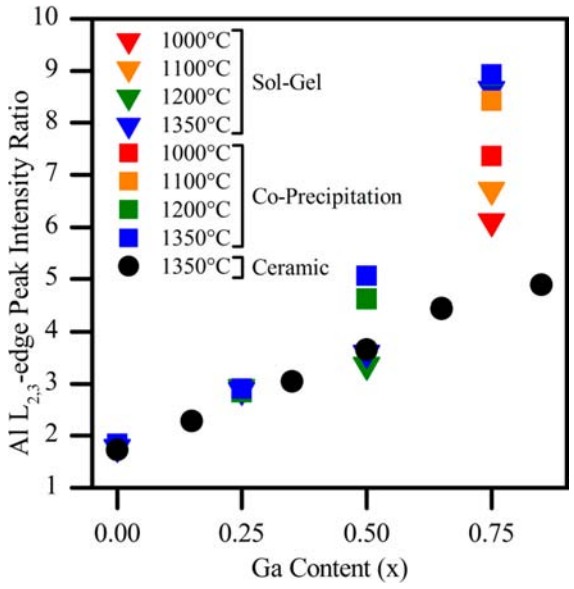

Figure 5. Octahedral peak intensity to tetrahedral peak intensity ratios (feature O:feature T) derived from Al $L_{2,3}$-edge XANES spectra from $Al_{1-x}Ga_xFeO_3$. Samples synthesized by the sol−gel method are shown as triangles; samples synthesized by the coprecipitation method are shown as squares; and samples synthesized via the ceramic method are shown as circles (determined from recently reported data).[17] The average Al coordination number increases with greater Ga content and with increasing annealing temperature.

are not quantitative, but do allow for a comparison of the different samples studied. It can also be seen from this comparison that, when $x \geq 0.50$, the samples prepared using the coprecipitation method have more Al in the octahedral site than the samples prepared via the sol−gel or ceramic methods. As well, samples synthesized via the coprecipitation method with low Al content (high Ga content) show a greater variance in the peak intensity ratios with changes in annealing temperature than samples produced using the sol−gel method. As will be discussed below, this suggests that there is greater ion mobility in the samples synthesized by the coprecipitation method, while the sol−gel and ceramic methods appear to suppress changes in the coordination of Al in this system with changes in annealing temperature.

3.2. Ga K-Edge XANES. The Ga K-edge XANES spectra from $Al_{1-x}Ga_xFeO_3$ synthesized by sol−gel and coprecipitation methods, and annealed at 1350 °C, are shown in Figure 6. These spectra result from 1s → 4p transitions and, similar to the Al $L_{2,3}$-edge XANES spectra (section 3.1), shift to higher energy with increasing coordination number.[17,38] Peak T corresponds to tetrahedrally coordinated Ga while peak O corresponds to octahedrally coordinated Ga, as has been shown by comparison of Ga K-edge XANES spectra from Ga_2S_3 (4-coordinate Ga), GaF_3 (6-coordinate Ga), and $Al_{2-x}Ga_xO_3$ (4- and 6-coordinate Ga).[17,38] Samples synthesized via the sol−gel method (Figure 6a) show negligible spectral changes when $x = 0.25$ and 0.50. As x increases above 0.50, the intensity of the tetrahedral feature decreases and the intensity of the octahedral feature increases. In comparison, spectra from samples formed via the coprecipitation method show changes between all four compositions studied, although the changes are less obvious between $x = 0.75$ and 1.00 due to issues with normalizing these spectra. Overall, these observations imply that Ga preferentially occupies the tetrahedral site when the Ga content is low and increasingly

dx.doi.org/10.1021/ic4007636 | Inorg. Chem. 2013, 52, 8612−8620

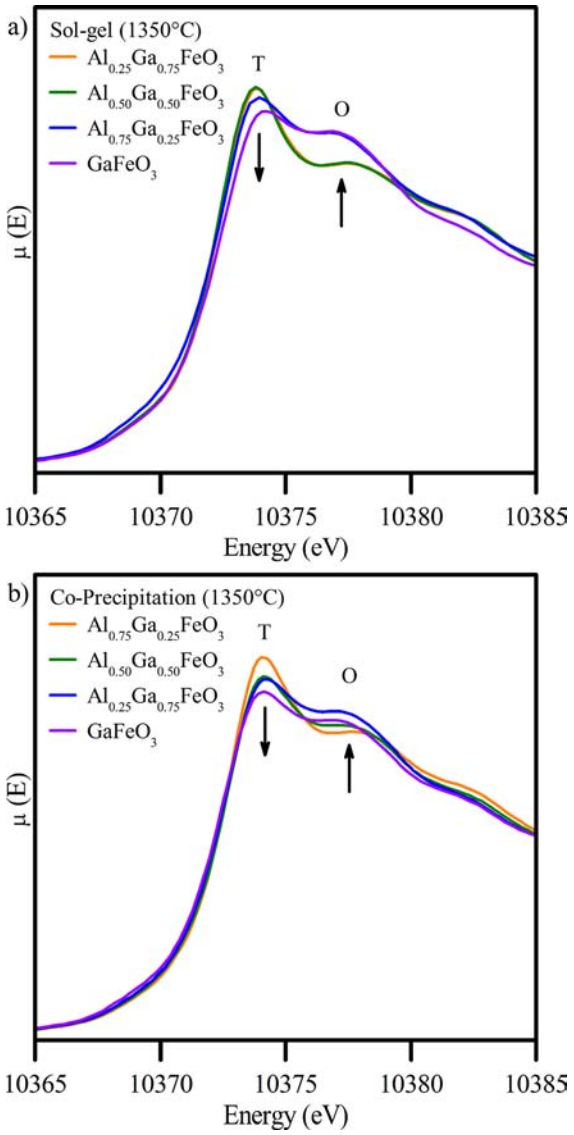

Figure 6. Normalized Ga K-edge XANES spectra are presented from $Al_{1-x}Ga_xFeO_3$ (x = 0.25, 0.50, 0.75, 1.00) synthesized using (a) the sol−gel method and (b) the coprecipitation method. All materials were annealed at 1350 °C. Arrows indicate the changes in intensity that occur with increasing Ga content. Ga preferentially occupies the tetrahedral site when the Ga content is low. With increasing Ga content, Ga occupies the tetrahedral site as before, and increasingly occupies the octahedral sites as well.

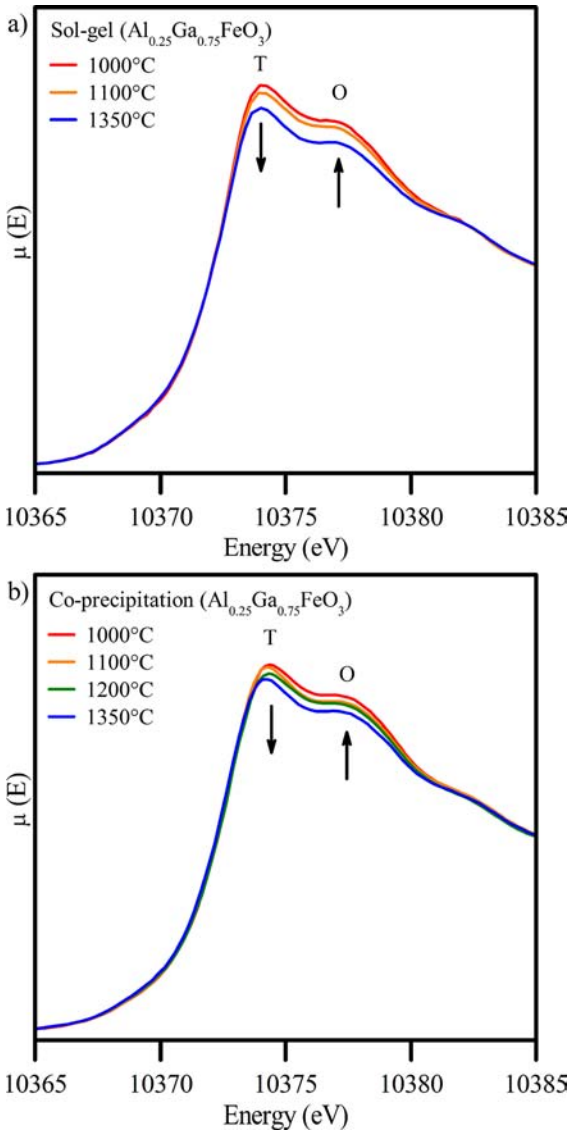

Figure 7. Normalized Ga K-edge XANES spectra are presented from $Al_{0.25}Ga_{0.75}FeO_3$ synthesized using (a) the sol−gel method and (b) the coprecipitation method, and annealed at multiple temperatures. Arrows indicate the relative changes in intensity of the two peaks that occur with increasing temperature. The decrease in the intensity of the tetrahedral feature (T) relative to the octahedral feature (O) indicates that Ga occupies the tetrahedral site more with increasing annealing temperature.

occupies the octahedral sites when the Ga concentration increases. This observation is in agreement with analysis of Ga K-edge XANES data from $Al_{1-x}Ga_xFeO_3$ synthesized via the ceramic method.[17]

The Ga K-edge spectra from $Al_{0.25}Ga_{0.75}FeO_3$ synthesized by sol−gel and coprecipitation methods, and annealed at different temperatures, are presented in Figure 7 (for additional stoichiometries see Figures S2 and S3 in the Supporting Information). The octahedral to tetrahedral peak intensity ratios (feature O:feature T) for the Ga K-edge spectra collected are shown in Figure 8 (the data from Figure 8 is also summarized in Tables S6−S8 in the Supporting Information). In comparison with the Al $L_{2,3}$-edge results, the Ga K-edge spectra show significantly smaller changes in the octahedral to tetrahedral peak intensity ratio with changes in annealing temperature. The peak intensity ratio changes very little with increasing annealing temperature; however, the overall intensity of tetrahedral and octahedral features decreased with increasing annealing temperature. (The overall decrease in intensity is thought to be due to changes in the density of unoccupied states as the materials become more crystalline, but is beyond the scope of this study and will not be discussed further.) The small variation in octahedral to tetrahedral peak intensity ratio indicates that the coordination environment of Ga changes very little with annealing temperature or synthetic method. That said, changes may be difficult to observe due differences in core-hole lifetime effects leading to a larger intrinsic line width for the Ga K-edge transition (1.82 eV) relative to the Al $L_{2,3}$-edge transition (0.004 eV).[39]

dx.doi.org/10.1021/ic4007636 | Inorg. Chem. 2013, 52, 8612−8620

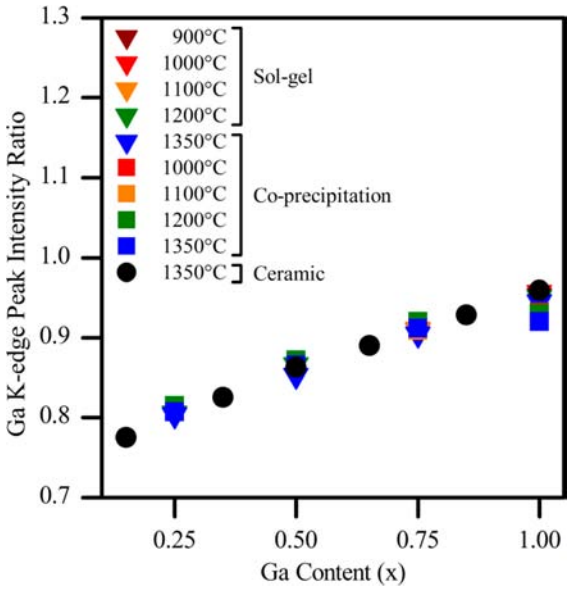

Figure 8. Octahedral peak intensity to tetrahedral peak intensity ratios (feature O:feature T) derived from Ga K-edge XANES spectra. $Al_{1-x}Ga_xFeO_3$ samples synthesized by the sol–gel method are shown as triangles; samples synthesized by the coprecipitation method are shown as squares; and samples synthesized via the ceramic method are shown as circles (determined from recently reported data).[17] The average coordination number of Ga increases with greater Ga content, but does not change significantly with synthetic method or annealing temperature.

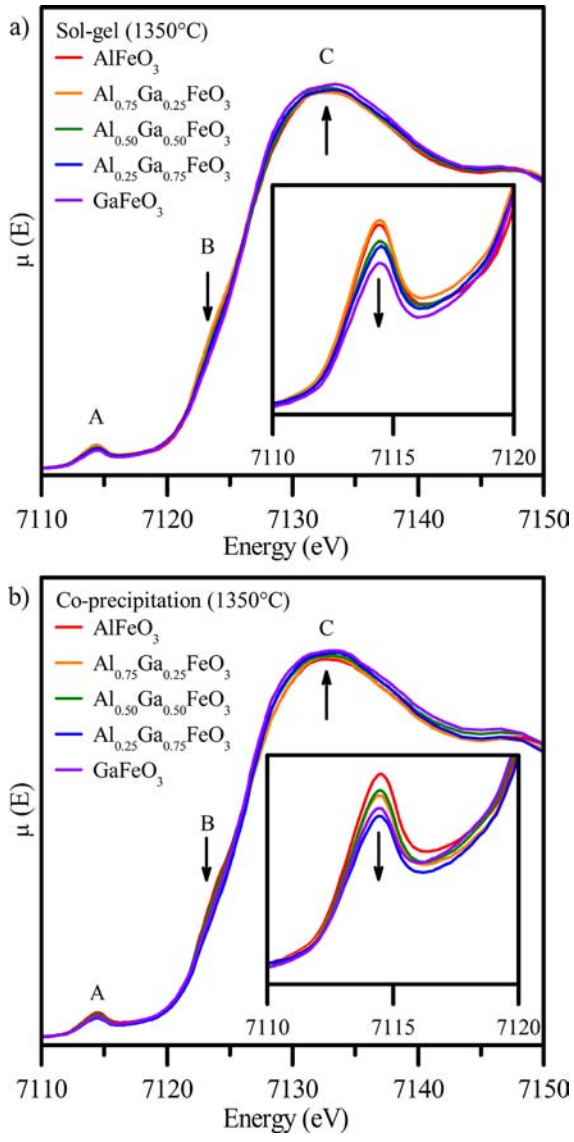

Figure 9. Normalized Fe K-edge XANES spectra from $Al_{1-x}Ga_xFeO_3$ (x = 0.00, 0.25, 0.50, 0.75, 1.00) synthesized using either (a) the sol–gel method or (b) the coprecipitation method. All materials presented were annealed at 1350 °C. An enlarged view of the pre-edge region is presented in the inset of each figure. Arrows indicate the change in intensity of the different features with increasing Ga content. With increasing Ga content, features A and B decrease in intensity, and feature C increases in intensity. This indicates that the average coordination number of Fe decreases as Ga is exchanged for Al in this system. (All Fe K-edge XANES spectra presented use the same y-axis scale to allow for comparison of intensities between figures.)

3.3. Fe K-Edge XANES. Normalized Fe K-edge XANES spectra from $Al_{1-x}Ga_xFeO_3$ samples synthesized by both the sol–gel and coprecipitation methods, and annealed at 1350 °C, are presented in Figure 9. The pre-edge feature centered at ~7114 eV is due to quadrupolar 1s → 3d transitions (feature A) while the main edge (>7120 eV) represents dipolar 1s → 4p transitions (features B and C).[40] The quadrupolar 1s → 3d transition is forbidden when Fe is in a centrosymmetric environment; however, inversion symmetry is lost as the coordination number decreases or when the octahedral environment around the metal center is distorted.[41] A decrease in coordination number (or distortion of the coordination environment) results in an increased overlap of the p- and d-states which increases the dipole character of the transition. As a result, the pre-edge intensity increases, making this feature very sensitive to the local Fe coordination environment.[17,40,41]

An expanded view of the pre-edge region of the $Al_{1-x}Ga_xFeO_3$ spectra is presented in the inset of Figure 9. Features A and B decrease in intensity while feature C increases in intensity with increasing Ga content for all samples studied regardless of synthetic method. The decrease in the intensity of the entire pre-edge region (feature A) as the Ga content is increased indicates that the average Fe coordination number increases. The intensities of features B and C have been shown to be related to the relative amount of 4- and 6-coordinate Fe present, for similar reasons as outlined for Al and Ga coordination number changes.[17] Thus, the decrease in feature B (tetrahedral) and the increase in the intensity of feature C (octahedral) also indicate an increase in the average coordination of Fe with increasing Ga concentration. A change in the main-edge region of Fe K-edge XANES spectra because of a change in the average Fe coordination number has also been observed in other oxide systems, including the Brownmillerite-phase oxides (e.g., $Ca_2M_xFe_{2-x}O_5$; M = Mn, Fe, Co, Al, Ga).[17,24,42]

Unlike the Al $L_{2,3}$-edge and Ga K-edge XANES spectra, the Fe K-edge spectra only indicate minor differences between synthetic methods. Figure 10 shows the comparison between $AlFeO_3$ and $GaFeO_3$ samples synthesized via the sol–gel, coprecipitation, and ceramic methods.[17] For both materials, the highest average Fe coordination number (lowest pre-edge intensity) is observed for samples synthesized via the ceramic method, followed by the sol–gel samples, and then the samples synthesized by a coprecipitation method. These differences are attributed to

dx.doi.org/10.1021/ic4007636 | Inorg. Chem. 2013, 52, 8612–8620

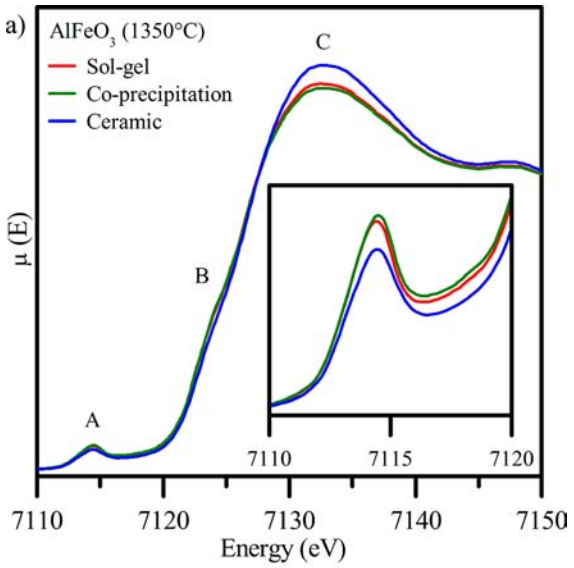

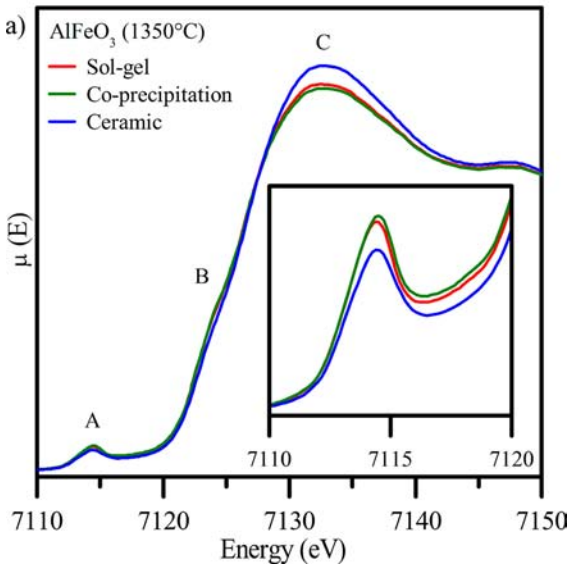

Figure 10. Normalized Fe K-edge XANES spectra are shown from (a) $AlFeO_3$ and (b) $GaFeO_3$ materials synthesized using the sol−gel, coprecipitation, or ceramic methods. All materials were annealed at 1350 °C. An enlarged view of the pre-edge region is presented in the inset of each figure. The intensity of features A and B is greatest for materials synthesized via the coprecipitation method, followed by the sol−gel method, followed by the ceramic method. The intensity of feature C shows the opposite trend, increasing in intensity as features A and B decrease in intensity. This shows that the average coordination number of Fe is highest in samples synthesized via the ceramic method and lowest in samples synthesized via the coprecipitation method. (All Fe K-edge XANES spectra presented use the same *y*-axis scale to allow for comparison of intensities between figures.)

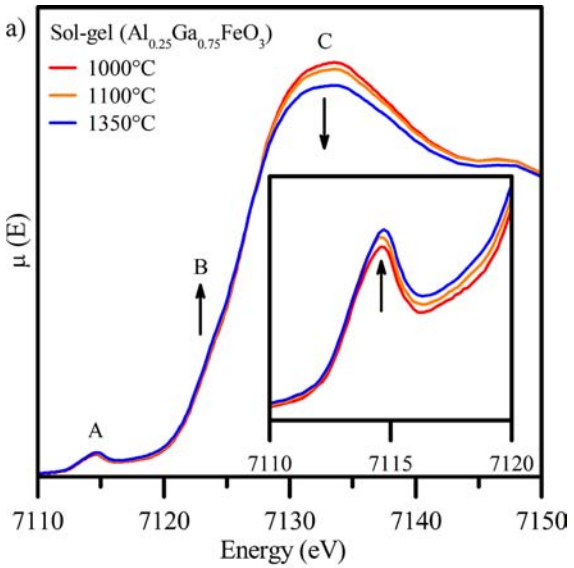

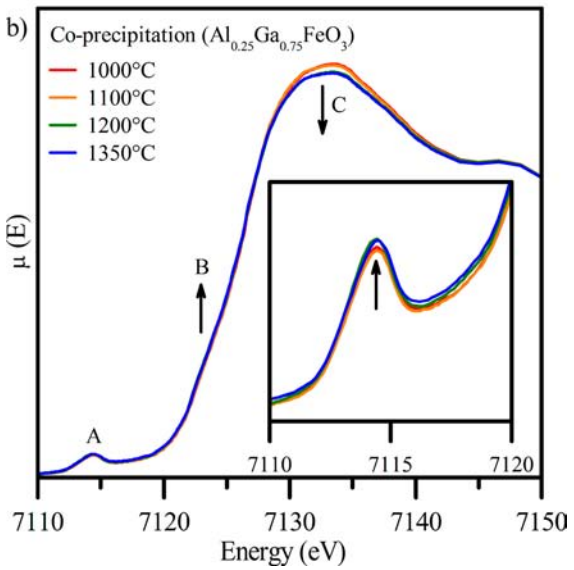

Figure 11. Normalized Fe K-edge XANES spectra are presented from $Al_{0.25}Ga_{0.75}FeO_3$ synthesized using (a) the sol−gel method or (b) the coprecipitation method and annealed at multiple temperatures. An enlarged view of the pre-edge region is presented in the inset of each figure. Arrows indicate how the spectral features change in intensity with increasing annealing temperature. Features A and B increase in intensity, and feature C decreases in intensity, with increasing annealing temperature. Therefore, Fe was found to increasingly occupy the tetrahedral site more when greater annealing temperatures were used during synthesis. (All Fe K-edge XANES spectra presented use the same *y*-axis scale to allow for comparison of intensities between figures.)

how the compounds form when using different synthetic methods, and will be discussed below.

Like the Al $L_{2,3}$-edge spectra, the Fe K-edge spectra of $Al_{0.25}Ga_{0.75}FeO_3$ synthesized by sol−gel and coprecipitation methods show changes in coordination with annealing temperature (Figure 11; see Figures S4 and S5 in the Supporting Information for additional stoichiometries). Regardless of composition or synthesis method, features A and B increase in intensity, and feature C decreases in intensity, with increasing annealing temperature. This indicates that the average coordination number of Fe decreases with increasing annealing temperature. As presented earlier, the average coordination number of Al increases with increasing annealing temperature while the average coordination number of Ga does not change significantly. Combined, these observations suggest that Al and Fe exchange sites with each other, and not with Ga, with increasing annealing temperature.

4. DISCUSSION

4.1. Changes in Coordination Number with Composition. The Al $L_{2,3}$-, Ga K- and Fe K-edge XANES experiments have shown that Al and Fe prefer to reside in octahedral sites while Ga prefers to reside in the tetrahedral site regardless of the

dx.doi.org/10.1021/ic4007636 | Inorg. Chem. 2013, 52, 8612−8620

synthetic method used to form these materials. This is consistent with experimental observations and theoretical predictions of octahedral site preference energies for these three cations.[17,22,43,44] It has been proposed that ionic radii, as well as the valence s- and p-states interacting with the anion, are the major factors determining site preference, with crystal field stabilization having a smaller contribution.[44−46] In the case of Ga, the complete electron d-shell poorly shields the nuclear charge, resulting in the s- and p-states experiencing a greater effective nuclear charge.[17,25,45] Thus, the 4s- and 4p-states of Ga are found at lower energies relative to the 3s- and 3p-states of Al.[25,45] The lower energy of the Ga 4s- and 4p-states leads to greater overlap with the O 2p-states, favoring a covalent Ga−O bond.[25] As the Al valence states are higher in energy than the Ga valence states, the Al 3s- and 3p-states do not overlap as effectively with the O 2p-states, favoring a more ionic bond.[25,45] As greater orbital overlap is favored in the smaller tetrahedral site, Ga preferentially occupies tetrahedral sites over Al or Fe.[43]

The site preference of Fe^{3+} can be difficult to predict without computation due to confounding factors such as magnetic interactions between sites, as well as the effect of the d-orbitals.[47] The Fe K-edge XANES spectra studied here indicate that Fe predominantly resides in octahedral sites and that the average coordination number of Fe increases as Ga replaces Al in the structure. This is due to the tetrahedral site preference of Ga, which inhibits Fe from occupying the tetrahedral site. In comparison, Al prefers to reside in octahedral sites and therefore competes with Fe for those sites, resulting in an increase in the amount of Fe present in the tetrahedral site when the Al concentration is high. As the amount of tetrahedrally coordinated Fe decreases with increasing Ga content, this indicates that there is greater antisite disorder in $AlFeO_3$ than in $GaFeO_3$, consistent with previously published results.[17]

4.2. Changes in Coordination Number with Annealing Temperature. It was observed that the average Al coordination number increased with increasing annealing temperature, while the average Fe coordination decreased. The average coordination number of Ga was not found to change significantly based on analysis of the Ga K-edge XANES spectra. However, analysis of the Fe K-edge XANES spectra indicates that slightly more 4-coordinate Fe was found in $GaFeO_3$ with increasing annealing temperature, which suggests that the average coordination number of Ga does in fact increase *slightly* with higher annealing temperatures. Overall, these observations indicate that Al and Fe exchange preferentially with each other and not with Ga. The strong tetrahedral site preference of Ga inhibits the ability of Fe or Al to displace it from the tetrahedral site, which explains why only negligible changes in the coordination number of Ga were observed with increasing annealing temperature.

4.3. Changes in Coordination Number with Synthetic Method. In the sol−gel process, the citric acid not only chelates the metals but also undergoes a condensation reaction with the ethylene glycol to produce a long-range polymeric network.[48] Thus, the more subtle changes in Al site occupancy for $Al_{1-x}Ga_xFeO_3$ samples produced by the sol−gel method, as compared to the coprecipitation method, are attributed to the organic network that is formed. This network could inhibit cation mobility during formation of the oxide. Conversely, in samples synthesized via the coprecipitation method, the metals are not bound in any sort of long-range network and should instead be a mix of metal cations and counteranions. Since there is no appreciable long-range network, cation diffusion should be faster, which explains the greater variation in the metal coordination number found in the materials produced using a coprecipitation method. In contrast, samples produced by the ceramic method have low ion mobility due to the energy required to break the metal oxygen bonds and for the metal cations to diffuse through the crystal lattice. Thus, samples prepared via the coprecipitation method show greater change in the coordination number of the metal atoms in $Al_{1-x}Ga_xFeO_3$ than those produced via either the sol−gel or ceramic methods.

5. CONCLUSION

A series of phase pure $Al_{1-x}Ga_xFeO_3$ samples have been successfully synthesized by the sol−gel and coprecipitation methods. These samples have been studied using XANES to determine changes in the average coordination number of Al, Ga, and Fe. It has been shown in this study that the synthetic method can play an important role in determining site occupancies, and that changes in composition have a greater effect than annealing temperature. Overall, it was found that Al and Fe prefer to reside in octahedral sites, while Ga has a strong tetrahedral site preference.[17] That said, it was also shown that the average coordination number of Al, and to a much lesser extent Ga, increases with increasing annealing temperature while the average coordination number of Fe decreases. This indicates that Al and Fe preferentially exchange sites with each other rather than with Ga, which is due to the strong tetrahedral site preference of Ga. Furthermore, it was found that samples synthesized via the coprecipitation method showed the greatest variability in metal coordination number. Samples synthesized via the sol−gel or ceramic methods also showed changes, but to a much smaller degree. The polymeric network formed during the sol−gel method and the oxide network present when materials are synthesized by the ceramic method are thought to inhibit the mobility of the ions during compound formation. In comparison, there is no long-range network restricting cation mobility for samples produced via the coprecipitation method, resulting in greater variations in coordination number. This study has demonstrated how changes in composition, annealing temperature, and synthetic method can affect metal site preference during synthesis. As the average coordination number of the metals will determine physical properties, this study also demonstrates how changes in synthetic method and composition could be used to selectively tailor the properties of the $Al_{1-x}Ga_xFeO_3$ system.

■ ASSOCIATED CONTENT

Supporting Information

Lattice constants, Al $L_{2,3}$- and Ga K-edge XANES peak intensity ratios, and additional Al $L_{2,3}$-, Ga K-, and Fe K-edge XANES spectra from materials synthesized using sol−gel and coprecipitation methods. This material is available free of charge via the Internet at http://pubs.acs.org.

■ AUTHOR INFORMATION

Corresponding Author

*E-mail: andrew.grosvenor@usask.ca Phone: (306) 966-4660 Fax: (306) 966-4730

Notes

The authors declare no competing financial interest.

■ ACKNOWLEDGMENTS

This project has been funded through a Discovery Grant awarded to A.P.G. from the Natural Sciences and Engineering

Research Council (NSERC) of Canada. J.D.S.W. also thanks the University of Saskatchewan for support. J. R. Hayes, E. R. Aluri, and M. N. Revoy from the Department of Chemistry, University of Saskatchewan, are thanked for help in the collection of the XANES spectra presented in this study. The Canadian Foundation for Innovation is thanked for funding the purchase of the PANalytical Empyrean powder X-ray diffractometer used in this work. Dr. Lucia Zuin and Ms. Isabelle Gauthier are thanked for help in using the 11ID-2 beamline at the CLS. The CLS is supported by NSERC, the National Research Council of Canada, the Canadian Institutes of Health Research, the Province of Saskatchewan, Western Economic Diversification Canada, and the University of Saskatchewan. Dr. Robert Gordon of the APS is thanked for help in using the 20-BM beamline. PNC/XSD facilities at the Advanced Photon Source and research at these facilities are supported by the US Department of Energy—Basic Energy Sciences, a Major Resources Support grant from NSERC, the University of Washington, the Canadian Light Source, and the Advanced Photon Source. Use of the Advanced Photon Source, an Office of Science User Facility operated for the U.S. Department of Energy (DOE) Office of Science by Argonne National Laboratory, was supported by the U.S. DOE under Contract No. DE-AC02-06CH11357.

REFERENCES

(1) Hill, N. A. *J. Phys. Chem. B* **2000**, *104*, 6694−6709.
(2) Fiebig, M.; Lottermoser, Th.; Fröhlich, D.; Goltsev, A. V.; Pisarev, R. V. *Nature* **2002**, *419*, 818−820.
(3) Eerenstein, W.; Mathur, N. D.; Scott, J. F. *Nature* **2006**, *442*, 759−765.
(4) Ogawa, Y.; Kaneko, Y.; He, J. P.; Yu, X. Z.; Arima, T.; Tokura, Y. *Phys. Rev. Lett.* **2004**, *92*, 047401.
(5) Kida, N.; Kaneko, Y.; He, J. P.; Matsubara, M.; Sato, H.; Arima, T.; Akoh, H.; Tokura, Y. *Phys. Rev. Lett.* **2006**, *96*, 167202.
(6) Remeika, J. P. *J. Appl. Phys.* **1960**, *31*, 263S−264S.
(7) Schieber, M.; Frankel, R. B.; Blum, N. A.; Foner, S. *J. Appl. Phys.* **1967**, *38*, 1282−1283.
(8) Naik, V. B.; Mahendiran, R. *J. Appl. Phys.* **2009**, *106*, 123910.
(9) Bouree, F.; Baudour, J. L.; Elbadraoui, E.; Musso, J.; Laurent, C.; Rousset, A. *Acta Crystallogr., Sect. B: Struct. Sci* **1996**, *B52*, 217−222.
(10) Arima, T.; Higashiyama, D.; Kaneko, Y.; He, J. P.; Goto, T.; Miyasaka, S.; Kimura, T.; Oikawa, K.; Kamiyama, T.; Kumai, R.; Tokura, Y. *Phys. Rev. B: Condens. Matter* **2004**, *70*, 064426.
(11) Momma, K.; Izumi, F. *J. Appl. Crystallogr.* **2008**, *41*, 653−658.
(12) Abrahams, S. C.; Reddy, J. M. *Phys. Rev. Lett.* **1964**, *13*, 688−690.
(13) Kim, W.; We, J. H.; Kim, S. J.; Kim, C. S. *J. Appl. Phys.* **2007**, *101*, 09M515.
(14) Szymański, K.; Dobrzyński, L.; Bakr, M.; Satuła, D.; Olszewski, W.; Parzych, G.; Fuess, H. *Phase Transitions* **2010**, *83*, 824−835.
(15) Roy, A.; Mukherjee, S.; Gupta, R.; Auluck, S.; Prasad, R.; Garg, A. *J. Phys.: Condens. Matter* **2011**, *23*, 325902.
(16) Saha, R.; Shireen, A.; Bera, A. K.; Shirodkar, S. N.; Sundarayya, Y.; Kalarikkal, N.; Yusuf, S. M.; Waghmare, U. V.; Sundaresan, A.; Rao, C. N. R. *J. Solid State Chem.* **2011**, *184*, 494−501.
(17) Walker, J. D. S.; Grosvenor, A. P. *J. Solid State Chem.* **2013**, *197*, 147−153.
(18) Mukherjee, S.; Garg, A.; Gupta, R. *J. Phys.: Condens. Matter* **2011**, *23*, 445403.
(19) Kaneko, Y.; Arima, T.; He, J. P.; Kumai, R.; Tokura, Y. *J. Magn. Magn. Mater.* **2004**, *304*, e769−e771.
(20) Kang, K. U.; Kim, S. B.; An, S. Y.; Cheong, S.-W.; Kim, C. S. *J. Magn. Magn. Mater.* **2006**, *272−276*, 555−556.
(21) Bakr Mohamed, M.; Senyshyna, A.; Ehrenberga, H.; Fuessa, H. *J. Alloys Compd.* **2010**, *492*, L20−L27.
(22) Han, M. J.; Ozaki, T.; Yu, J. *Phys. Rev. B: Condens. Matter* **2007**, *75*, 060404.
(23) Kim, J.-Y.; Koo, T. Y.; Park, J.-H. *Phys. Rev. Lett.* **2006**, *96*, 047205.
(24) Grosvenor, A. P.; Greedan, J. E. *J. Phys. Chem. C* **2009**, *113*, 11366−11372.
(25) Grosvenor, A. P.; Ramezanipour, F.; Derakhshan, S.; Maunders, C.; Botton, G. A.; Greedan, J. E. *J. Mater. Chem.* **2009**, *19*, 9213−9220.
(26) Berbenni, V.; Milanese, C.; Bruni, G.; Marini, A. *J. Therm. Anal. Calorim.* **2005**, *82*, 401−407.
(27) Majzlan, J.; Navrotsky, A.; Evans, B. J. *Phys. Chem. Miner.* **2002**, *29*, 515−526.
(28) Bhushan, B.; Mukherjee, S.; Basumallick, A.; Bandopadhyay, S. K.; Das, D. *Hyperfine Interact.* **2008**, *187*, 101−107.
(29) *X'Pert Highscore Plus Program, Version 3.0e*; PANalytical B.V.: Almelo, The Netherlands, 2012.
(30) Shannon, R. D. *Acta Crystallogr., Sect. A: Found. Crystallogr.* **1976**, *32*, 751−767.
(31) Denton, A. R.; Ashcroft, N. W. *Phys. Rev. A: At., Mol., Opt. Phys.* **1991**, *43*, 3161−3164.
(32) Hu, Y. F.; Zuin, L.; Reininger, R.; Sham, T. K. *AIP Conf. Proc.* **2007**, *879*, 535−538.
(33) Thompson, A.; Attwood, D.; Gullikson, E.; Howells, M.; Kim, K.-J.; Kirz, J.; Kortright, J.; Lindau, I.; Pianetta, P.; Robinson, A.; Scofield, J.; Underwood, J.; Vaughan, D.; Williams, G.; Winick, H. *X-ray Data Booklet*, 3rd ed.; Lawrence Berkeley National Laboratory: Berkeley, 2009.
(34) Heald, S. M.; Brewe, D. L.; Stern, E. A.; Kim, K. H.; Brown, F. C.; Jiang, D. T.; Crozier, E. D.; Gordon, R. A. *J. Synchrotron Radiat.* **1999**, *6*, 347−349.
(35) Ravel, B.; Newville, M. *J. Synchrotron Radiat.* **2005**, *12*, 537−541.
(36) van Bokhoven, J. A.; Nabi, T.; Sambe, H.; Ramaker, D. E.; Koningsberger, D. C. *J. Phys.: Condens. Matter* **2001**, *13*, 10247−10260.
(37) Weigel, C.; Calas, G.; Cormier, L.; Galoisy, L.; Henderson, G. S. *J. Phys.: Condens. Matter* **2008**, *20*, 135219.
(38) Nishi, K.; Shimizu, K.-I.; Takamatsu, M.; Yoshida, H.; Satsuma, A.; Tanaka, T.; Yoshida, S.; Hattori, T. *J. Phys. Chem. B* **1998**, *102*, 10190−10195.
(39) Krause, M. O.; Oliver, J. H. *J. Phys. Chem. Ref. Data* **1979**, *8*, 329−350.
(40) Westre, T. E.; Kennepohl, P.; DeWitt, J. G.; Hedman, B.; Hodgson, K. O.; Solomon, E. I. *J. Am. Chem. Soc.* **1997**, *119*, 6297−6314.
(41) de Groot, F. *Chem. Rev.* **2001**, *101*, 1779−1808.
(42) Gaultois, M. W.; Greedan, J. E.; Grosvenor, A. P. *J. Electron Spectrosc. Relat. Phenom.* **2011**, 192−195.
(43) Miller, A. *J. Appl. Phys.* **1959**, *30*, 24S−25S.
(44) Price, G. D.; Price, S. L.; Burdett, J. K. *Phys. Chem. Miner.* **1982**, *8*, 69−76.
(45) Goodenough, J. B.; Loeb, A. L. *Phys. Rev.* **1955**, *98*, 391−408.
(46) Burdett, J. K.; Price, G. D.; Price, S. L. *J. Am. Chem. Soc.* **1982**, *104*, 92−95.
(47) de Groot, F. *Coord. Chem. Rev.* **2005**, *249*, 31−63.
(48) Cushing, B. L.; Kolesnichenko, V. L.; O'Connor, C. J. *Chem. Rev.* **2004**, *104*, 3893−3946.